Physica D 49 (1991) 161–169
North-Holland

Turing-type chemical patterns in the chlorite–iodide–malonic acid reaction

P. De Kepper, V. Castets, E. Dulos and J. Boissonade
Centre de Recherche Paul Pascal, Université Bordeaux I, Avenue Schweitzer, 33600 Pessac, France

We describe experimental observations of symmetry breaking stationary patterns. These patterns are interpreted as the first unambiguous evidence of Turing-type structures in a single-phase isothermal chemical reaction system. Experiments are conducted with the versatile chlorite–iodide–malonic acid reaction in open spatial reactors filled with hydrogel. A phase diagram gathering the domain of existence of symmetry breaking and no-symmetry breaking standing patterns is discussed.

1. Introduction

Recently several types of open spatial reactors have been designed to produce sustained spatio-temporal structures [1–7]. In these reactors the experiments are no longer limited to the rapid determination of some transient triggered wave properties in excitable media [8–12]. Many other asymptotic spatio-temporal behaviors can be reproducibly attained and controlled. Furthermore, these reactors make a larger number of chemically different oscillating and bistable reactions [13, 14] amenable for spatial studies. This tremendously increases the likehood of uncovering, in the field of chemistry, many new types of spatial self-organization phenomena [15, 16] besides the classic triggered waves. A rejuvenation of experimental studies of spatial self-organization phenomena in chemical systems has just started. Though a number of these studies are still based on the classical excitable properties of the popular Belousov–Zhabotinsky (BZ) reaction [2–4], other previously undocumented wave-like [5–7] and standing [6, 7] concentration patterns have been discovered.

In a previous paper [17], we reported the first clear evidence of a Turing structure [18] in an isothermal single phase reaction system. Here, we shall further elaborate on these observations and show how these Turing structures are closely associated with the emergence of standing front patterns organized parallel to the feed boundaries.

Let us first make clear what we mean by the term "Turing structures" and briefly enumerate the main properties of these structures: (a) They are *stationary* concentration patterns, originating solely from the coupling of *reaction* and *diffusion* processes. In particular, patterns associated with any type of hydrodynamic motion are excluded. Seemingly unmoving patterns, called "mosaic structures", were reported to develop in a number of different oscillating and even monotonic reactions [19, 20] when the reacting solutions were spread in a thin layer of free fluid. At one time thought of as examples of standing patterns resulting from a reaction–diffusion instability, they are now considered merely the result of convective instabilities induced by adverse density gradients of different origins, i.e., surface evaporative cooling of solvent, specific partial volume changes between reagents and products, since convective motions have actually been observed in a few cases [21, 22]. (b) The patterns result from *spontaneous symmetry breaking* phenomena associated with steady state instabilities. The symmetry breaking is defined in comparison with the boundary condition geometry. (c) The patterns are characterized, at the transition, by an *intrinsic* wavelength which does not depend on

0167-2789/91/$03.50

the geometrical parameters of the system but only on the concentrations or input rates of the reactants, the diffusion coefficients, and the macroscopic reaction rates. This distinguishes the Turing patterns from other well known nonequilibrium structures like the convective Bénard cells or the Taylor vortices in Couette flows, which depend on some geometric length of the system [23]. In Turing patterns, the size of the system is important only when the system is smaller than a few wavelengths – due to the necessary fit with the boundary conditions – but disappears for larger systems. Geometry, nonetheless, can play an important role in the pattern selection mechanisms at finite distance from the bifurcation values [24].

2. Experimental technique

2.1. The gel strip reactor

The reactor is made of a narrow flat piece of polyacrylamide hydrogel. This transparent, relatively inert gel avoids any advective fluid motion inside the reaction cell. Two types of reactor geometry are currently used in the experimentation. One is a rectangular strip 20 mm long; the other (fig. 1) is an annular strip with 42 mm outer diameter. In both cases the strips have a width of 3 mm and a thickness of 1 mm. These porous strips are squeezed between a white "Ertalite" bottom plate and a glass or plexiglass cover which allows for observations from the top. Monitoring is provided by a CCD camera. Images are usually stored on video tapes and ultimately processed on a NUMELEC (Pericolor 2000) image analyzer. The long edges (or the rims) of the gel are set in contact with the content of two vigorously stirred tanks (fig. 1) where chemical compositions are kept constant by continuous flow of fresh solutions. The feed of the tanks is provided by peristaltic pumps which show less than 2% flow-rate drifts over 24 h. The thermoregulation of the system and the precooling of input flows are

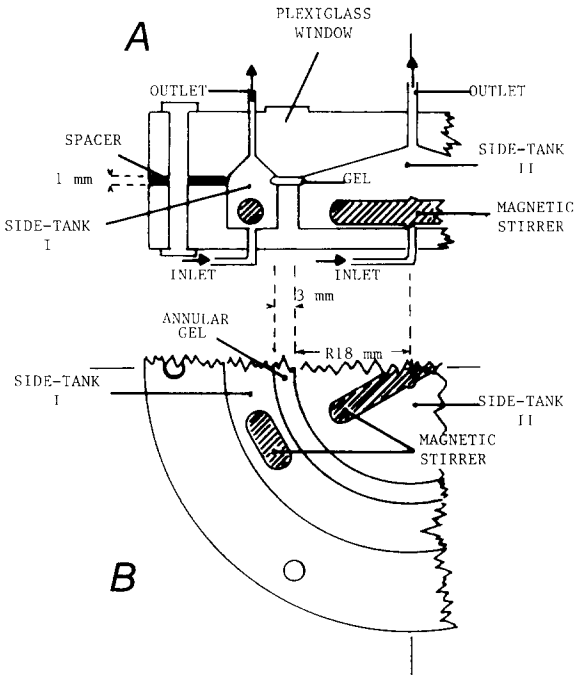

Fig. 1. Sketch of the annular gel strip reactor. (a) Cross-section (half part); (b) top view (quarter part).

performed by a waterjacket; the temperature is maintained at 7.0 ± 0.4°C.

2.2. The gel preparation

The hydrogel is prepared by dissolving in a 100 ml deionized water solution: 17.7 g acrylamide, 0.10 g N,N'-methylene-bisacrylamide, 0.7 g ammonium persulfate, 1.0 g triethanolamine, and 2.8 g Thiodène (a soluble starch from PROLABO used as triiodide (I_3^-) color indicator). The polymerizing solution is spread to form a thin film and left to react for 1 h. The whole preparation is performed at 0°C. The resulting sheet of polymer is then thoroughly washed and set to swell in purified water for at least 24 h before the reactor strip is cut out. During the swelling, the volume of the gel increases by a factor of three. The dry weight of the polymer is 5% of the wet gel. The average pore size, determined by the standard light scattering technique, is about 60 Å. Our hydrogel is thus essentially water in a loose grid

matrix of polymer, so that the diffusion of small species should not differ much from that found in pure water.

2.3. The reaction

The chemical reaction selected for our study is the chlorite (ClO_2^-)–iodide (I^-)–malonic acid (MA) oscillatory reaction. It has played an essential role in the development of oscillating and stationary chemical front structures [6, 7] in "Couette reactors", which are quasi-one-dimensional open spatial reactors. This reaction is among the very few which can both exhibit transient oscillatory behavior in a batch stirred reactor [25, 26] and trigger waves, if solutions are poured in a thin layer onto a petri dish [25]. Kinetic studies by Lengyel et al. [26] have shown that the batch oscillatory behavior of this system is linked to that of the more recently discovered chlorine dioxide (ClO_2)–iodine (I_2)–malonic acid (MA) oscillatory reaction for which a skeleton mechanism has been proposed [26]. In this model, the strongly self-inhibited reaction between chlorite and iodide plays a fundamental part in controlling the switching between a slow iodide producing and a fast iodide consuming processes.

2.4. The experimental procedure

Fresh chemicals are stored in three separate flasks containing respectively a basic sodium chlorite solution, a neutral iodide solution, and a solution of malonic and sulphuric acids. They are pumped and mixed into the stirred tanks, on each side of the gel strip, as follows: chlorite and iodide solutions on one side (side I), malonic acid and iodide solutions on the other side (side II). Notice that, at large pH values, the reaction between chlorite and iodide is very slow [27]; in our conditions, no significant reaction is observed after 3 h. The residence time in each side-tank is fixed at 15 min. With this feeding mode, neither of the solutions in the side-tanks is significantly reactive on its own and uniform compositions are easily achieved along the edges of the gel strip. In this paper, the chemical parameter values $[X]_0$ correspond to the concentration of species X in the stirred side-tanks. Experiments are usually started by flowing simultaneously premixed solutions of chemicals in each side-tank. Chemical gradients and patterns are allowed to settle spontaneously. Each composition is maintained for at least 6 h. A number of test experiments operated over 36 h show no significant difference with the pattern organization obtained after the first 6 h, save some fading of the color contrast probably due to the slow hydrolysis of the starch indicator.

3. Experimental results

Our feed conditions, where the chlorite (the oxidant) is fed only along one edge of the gel, lead to a monotonically decreasing oxidation capacity of the solution in the gel reactor from edge I to the malonic acid (a reducer) rich edge II. Iso-oxidation capacity lines then naturally build up parallel to the feed boundaries.

During the set of experiments reported here, the chlorite, the base, and the sulphuric acid concentrations were kept unchanged. For the fixed value of $[MA]_0 = 1.0 \times 10^{-2}$ M and increasing iodide feed concentrations, the sequence of stationary patterns shown in figs. 2a–2c was obtained. At low $[I^-]_0$ (fig. 2a), a single stable sharp color change was observed between the two edges. This trivial concentration pattern, which develops parallel to the feed boundaries, corresponds to a continuous increase in $[I_3^-]$ from edge I, where iodine species are mainly present as IO_3^- and HIO_2, to edge II, where the iodine species are mainly present as iodide, iodine, and triiodide. The local sharp change of color reveals the formation of a stable chemical front. This front is associated with the well known autocatalytic switching mechanism [28] of the chlorite–iodide reaction which, in particular, leads to a sharp decrease of the iodide concentration, by several orders of magnitude.

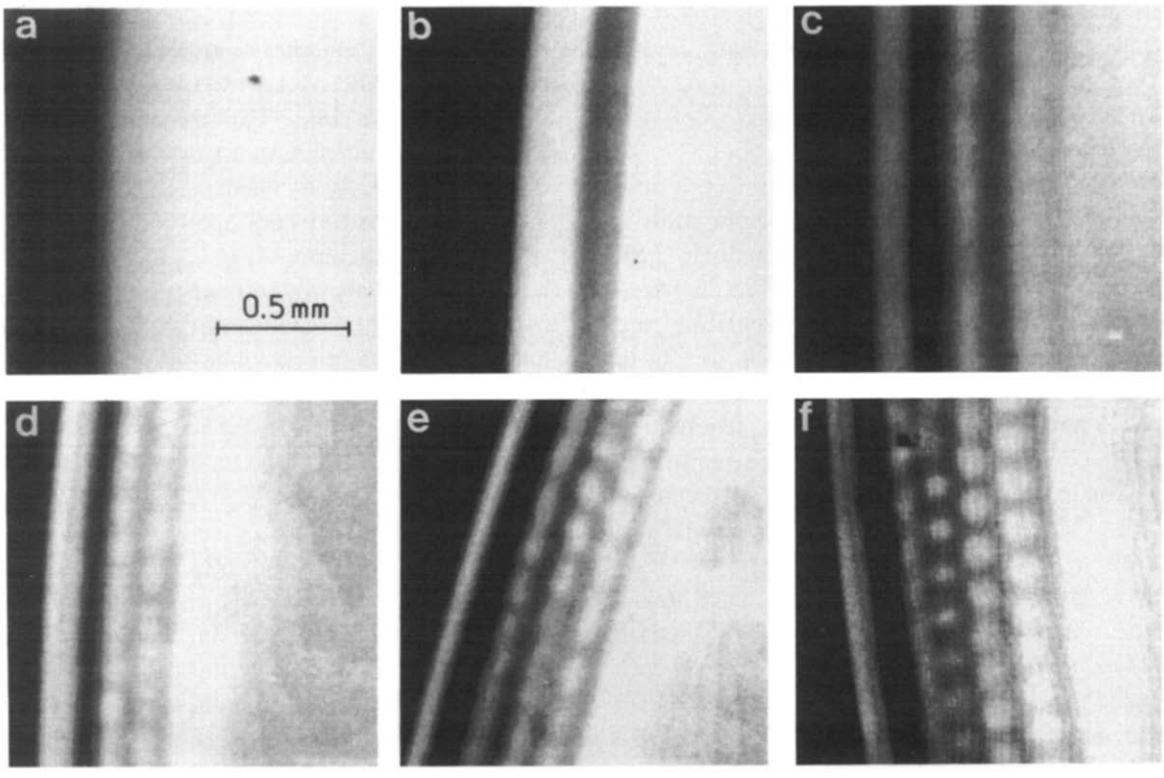

Fig. 2. Sustained chemical patterns in the annular gel strip reactor. Contrast enhanced images of the central portion of the reactor: Dark regions correspond to reduced iodine states colored in blue by the starch–triiodide complex, clear zones correspond to oxidized iodine states. The slight curvature of the first dark front (on the left of each image) is due to the circular geometry of the reactor. All other structures develop parallel to this front. All pictures are at the same scale and set so that edges I and II correspond respectively to the right- and left-hand sides of the pictures. Experimental conditions were as follows. Temperature: 4°C. Boundary feed compositions: fixed concentrations: $[H_2SO_4]_0^I = 1 \times 10^{-2}$ mol//, $[NaClO_2]_0^{II} = 2.4 \times 10^{-2}$ mol//, $[NaOH]_0^{I,II} = 3 \times 10^{-3}$ mol//, $[Na_2SO_4]_0^{I,II} = 3 \times 10^{-3}$ mol// with $[CH_2(COOH)_2]_0^I$: (a, b, c) 3.3×10^{-3} mol//; (d, e, f) 8.3×10^{-3} mol//, and $[I^-]_0^{I,II}$: (a) Single stationary font; 1.0×10^{-3} mol//. (b) Stationary triple-front structure; 1.33×10^{-3} mol//. (c) Multiple stationary band pattern; 1.66×10^{-3} mol//. (d) Fuzzy modulated band pattern; 1.33×10^{-3} mol//. (e) Triple-line spot pattern (Turing structure); 1.66×10^{-3} mol//. (f) Quadruple-line spot pattern (Turing structure); 2.66×10^{-3} mol//.

On increasing $[I^-]_0$, a first nontrivial concentration pattern forms. It consists in the development, parallel to the previous sharp front, of a thin dark (reduced iodine) band in the clearer (oxidized iodine) region (fig. 2b). This stationary structure is similar to that previously observed in the Couette reactor with asymmetric boundary feed conditions [6, 7]. In this latter reactor the diffusive transport process is provided by small scale turbulent mixing. The effective diffusion coefficient, identical for all species in the solution, is then of the order of 0.1 $cm^2\ s^{-1}$ and the characteristic spacing between bands is typically 20 mm. In our present gel reactors, the typical distance between bands is 0.2 mm. Assuming that in the two experiments, the characteristic reaction times are of the same order of magnitude, we have the following approximation: $l_1/l_2 \sim (D_1/D_2)^{1/2}$, where the l_i's and D_i's are respectively the characteristic lengths and associated average diffusion coefficients of the two systems. This leads to an estimate of diffusion coefficients in the gel experiments of the order of 10^{-5} $cm^2\ s^{-1}$, which is typically what is found for small ionic species in free aqueous solution. On further increasing $[I^-]_0$, up to three additional dimmer

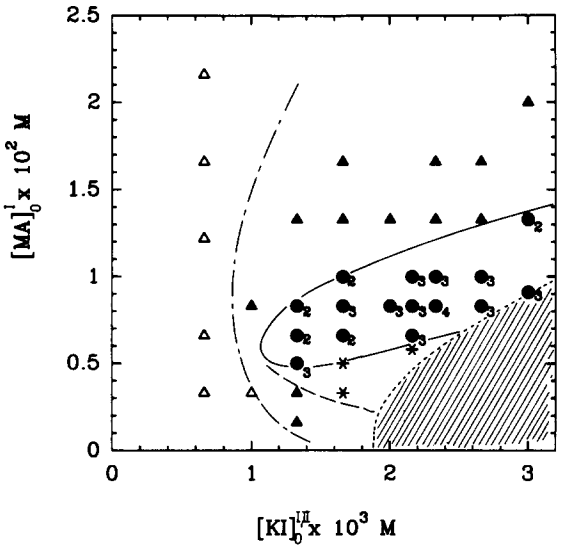

Fig. 3. Spatial structures phase diagram in the (iodide, malonic acid) constraint space. Fixed constraints as in fig. 2. (△) Single stationary front structure (fig. 2a); (▲) stationary triple-front structure (fig. 2b); (∗) stationary multiple-band pattern (fig. 2c); (●) Turing structures (figs. 2d, 2e, 2f). Hatched region correspond to a domain where iodine precipitates are observed.

dark bands develop parallel to the feed boundaries, in the oxidized region (fig. 2c).

At higher malonic acid concentration (e.g. $[MA]_0 = 2.0 \times 10^{-2}$ M), another completely new type of pattern is observed beyond a critical value of $[I^-]_0$ (figs. 2d–2f). Ranges of clear spots develop in the direction parallel to the feed boundaries. Indeed, all the previous bands – except the first clear one starting from reservoir II – lose their azimuthal invariance and break into rows of clear spots in a slightly darker background. This is a genuine *spontaneous symmetry breaking* phenomenon relative to the boundary feed geometry. As shown in the sequence of pictures (figs. 2d–2f) these structures become more easily discernible with increasing $[I^-]_0$. The spot patterns develop over large regions of the reactor, often extending over the full length of the reactor.

As shown in the phase diagram (fig. 3), the region where these symmetry breaking patterns are clearly observed is surrounded by regions where at least three stationary front structures are obtained. Along the transition line, spot patterns often shear the space with regions of fuzzy band structures. As the iodide concentration is further increased, away from the transition line, the extension of the spot regions readily grows at the expense of the plain stripe structure. Inside the domain where the spot structure is observed, the number of visible rows of spots varies; the figures next to the symbols (fig. 3) stand for the number of clearly visible lines of spots. At high $[I^-]_0$ values, iodine crystals are observed to form along the first sharp stationary front along side I and obscures the neighbouring concentration patterns (hatched domain in fig. 3). Within our present experimental accuracy, the patterns appear and disappear reproducibly, without hysteresis, as a function of the control parameters. The sharpness of the spot patterns increases as the control parameter values move away from the transition line. An accurate detailed study of the bifurcation to the patterns is presently out of reach because of the weak color contrast due to the low concentration of colored species. Fig. 4 presents an example of the periodic light intensity profile observed parallel to the feed edges. Though there are some irregularities in the intensity modulations, the patterns have a well defined wavelength λ, in this case $\lambda \simeq 0.17$ mm. The wavelength of these longitudinal structures seems intrinsic. The development of these structures

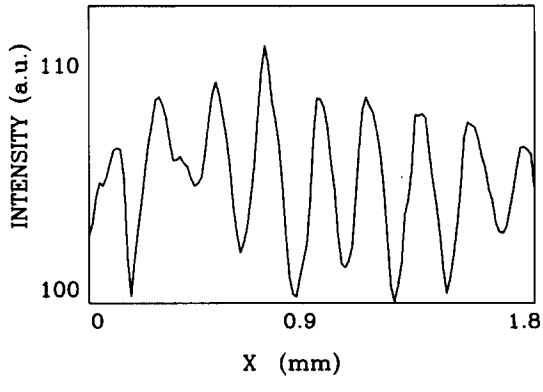

Fig. 4. Light intensity profile along the line of spot structures, parallel to the feed boundaries of the gel strip reactor. Experimental conditions as in fig. 2f.

does not sensitively depend on whether they are performed in the circular (periodic boundary conditions) or in a rectangular reactor (no flux boundary conditions). Their characteristic wavelength is not related to any of the geometric dimensions of the reactors including the thickness $\geq 5\lambda$. In the explored (iodide, malonic acid) section of the phase diagram, the wavelength of this transverse pattern does not change by more than 15%. Taking into account all the abovementioned properties, the structures formed of lines of stationary periodic concentration profiles, parallel to the feed edges, meet all the requirements of Turing patterns: stationarity, spontaneous symmetry breaking, intrinsic wavelength.

4. Discussion

The necessary conditions for Turing patterns are stringent. First, the kinetics should include at least one positive feedback loop (e.g. autocatalysis or substrate inhibition) and at least one negative feedback process (e.g., back inhibition). Oscillatory reactions necessarily fulfill this prerequisite. Though there is not yet a good detailed reaction scheme for the chlorite–iodide–malonic acid reaction, kinetic mechanisms of a number of subreaction systems are now well established [26–28].

Secondly, the major positive feedback species must diffuse significantly slower than the main negative feedback species. Of particular interest to us are the calculations by Lengyel and Epstein [29] using a two-variable skeleton model of the ClO_2–I_2–MA reaction. They show that, in this subsystem, a Turing instability would occur if I^- (the species controlling the positive feedback loop) diffuses slower than ClO_2^- (the species controlling the negative feedback process). It is still unclear if the natural small difference in the diffusion coefficients between these species (or other intermediate species of the reaction), in aqueous solution, is sufficient to trigger the onset of a Turing instability. Some theoretical studies show that, under particular conditions, these differences may be arbitrarily small [30, 31]. Another possibility is an enhancement of the difference in the diffusion coefficients due to diffusion processes in the gel. Species that preferentially adsorb on specific sites of the polymer matrix would exhibit weaker apparent diffusion coefficients. Such trapping sites for I_3^- and I_2 could be provided by the immobilized starch. However, the Turing structures have recently been shown to develop even in the absence of starch [32]. Adsorption sites could also be provided by the amide functions on the gel; though the polymer only represents 5% by weight of the hydrogel, the concentration of amide function is as high as 0.7 M, which is much greater than any other species in the system. Diffusion and adsorption measurements of different species in the gel are presently in progress in order to better characterize the origin of the observed Turing structures. It is also stimulating to notice that, the domain of Turing instability recently calculated by Lengyel and Epstein [29] on a model of the ClO_2–I_2–MA, qualitatively develops as in our phase diagram (fig. 3): At constant oxidant concentration, the region of Turing structures grows in the direction of increasing malonic acid and iodine species concentration [29]. Our latest experiments show that Turing structures can indeed be produced with the ClO_2–I_2–MA reaction [33].

One must also bear in mind that, in all cases, the reported observations are based on top views of the patterns. Thus, taking into account the characteristic dimensions of the different structures in comparison with the size of the gel strip, the representations on fig. 2 correspond, in fact, to two-dimensional projections of actually three-dimensional structures. In the region where the Turing-type patterns clearly develop over three or more lines (figs. 2e, 2f) the projections usually fit with a body-centered cubic pattern in agreement with the most stable three dimension Turing patterns predicted by Walgraef et al. [34]. A number of defects in the regular hexagonal arrangement

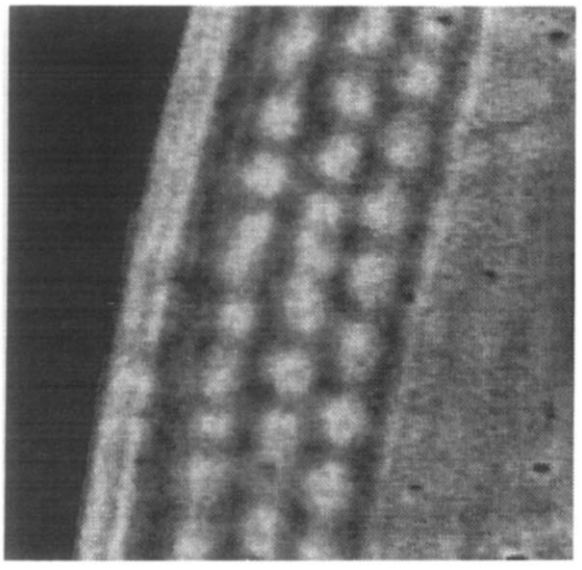

Fig. 5. Example of a fully developed irregular Turing structure. Notice the distortion of the regular hexagonal arrangement. Experimental conditions as in fig. 2 with $[CH_2(COOH)_2]_0^I = 9 \times 10^{-3}$ mol/ℓ; $[I^-]_0^{I,II} = 3 \times 10^{-3}$ mol/ℓ.

can also be seen from place to place along the region of spot patterns as exemplified in fig. 5. This could be due to some inherent small inhomogeneities of gels or to poorly controlled boundary conditions. Yet some preliminary calculations of Turing patterns in a two-dimensional reaction–diffusion system, with transverse concentration gradients introduced to mimic the experiments, show the same type of defects [35]. Taking into account that the side-tanks are thoroughly mixed and contain nonreactive solutions, and that the size of the gel inhomogeneities is several orders of magnitude smaller than the wavelength of the patterns, we think rather that the experimentally observed dislocations are also a direct consequence of the externally driven composition gradients.

Though the most spectacular result of the above experiments is the formation of the symmetry breaking patterns, the band patterns also merit some attention. The origin of these multiple band structures is still unclear. They could correspond to steep front structures induced by the imposed asymmetric boundary feed conditions, as discussed by Arneodo and Elezgaray [31, 36]. The formation of these stiff standing front structures does not require any differences in the diffusion coefficients of the species. They are not directly related to the Turing-type structures. However, stationary band patterns with more than three stationary fronts have never been observed in a Couette reactor where the effective diffusion coefficients of all species are forced to strict equality by the turbulent diffusion process [37]. This could mean that they also require some differences in the diffusion coefficients. Theoretical calculations by Dewel et al. [38] on patterning phenomena in strongly anisotropic media suggest that these band structures could still result from a Turing instability, which initially develops only in one direction. Experimentally, this case would be very difficult to distinguish from the previous one. One more possibility is that some of these band structures (beyond the third front starting from side II) are an illusion due to the stacking of different planes of spot structures which, for some region of parameter space, arrange themselves in a staggered way so that, on the average, they are only viewed as lines of different intensities.

5. Conclusion

As initially suggested by one of us [39] and further emphasized by Arneodo et al. [31], the approach to Turing structures in confined systems by introducing chemical gradients has been a successful method. Iodine–oxychlorine reaction systems [40] have now gained a rather unique status among isothermal oscillating and bistable reactions in liquid phase. Thus, to evaluate the full significance of this method, other reactions should be tested in the future. In this respect, the formidable expansion, during the last decade, in the design of homogeneous oscillating reactions should favor the discovery of Turing structures in other similar chemical systems.

Since biological systems are naturally gradient driven systems due to their feeding through membranes, attention should now be turned to the problem of pattern formation in nonuniform media instead of the more traditional space-uniform feed hypothesized in most theoretical calculations [15, 16, 41, 42].

Acknowledgements

We are indebted to A. Arneodo, P. Borckmans, G. Dewel and Q. Ouyang for stimulating discussions, and to I. Lengyel and I.R. Epstein for making their results available prior to publication. This work has been supported by the Venture Research Unit of British Petroleum.

References

[1] J. Boissonade, in: Dynamic and Stochastic Processes. Theory and Applications, eds. R. Lima, L. Streit and R. Vilela-Mendes, Lecture Notes in Physics, No. 355 (Springer, Berlin, 1990) p. 76.

[2] W.Y. Tam, W. Horsthemke, Z. Noszticzius and H.L. Swiney, J. Chem. Phys. 88 (1987) 3395;
G. Skinner and H.L. Swiney, Physica D 40 (1991) 1–16;
G. Kshirsagar, Z. Noszticzius, W.D. McCormick and H.L. Swinney, Physica D 49 (1991) 5–12, these Proceedings.

[3] Z. Noszticzius, W. Horsthemke, W.D. McCormick, H.L. Swinney and W.Y. Tam, Nature 329 (1987) 619;
N. Kreisberg, W.D. McCormick and H.L. Swinney, J. Chem. Phys. 91 (1989) 6532.

[4] E. Dulos, J. Boissonade and P. De Kepper, in: Nonlinear Wave Processes in Excitable Media, eds. A.V. Holden, M. Markus and H.G. Othmer (Plenum, New York, 1990) pp. 423–433.

[5] W.Y. Tam, J.A. Vastano, H.L. Swinney and W. Horsthemke, Phys. Rev. Lett. 61 (1988) 2163;
W.Y. Tam and H.L. Swinney, Physica D 46 (1990) 10.

[6] Q. Ouyang, J. Boissonade, J.C. Roux and P. De Kepper, Phys. Lett. A 134 (1989) 282;
P. De Kepper, Q. Ouyang, J. Boissonade and J.C. Roux, in: Dynamics of Exotic Phenomena in Chemistry, eds. M. Beck and E. Körös, Reac. Kinet. Catal. Lett. (Budapest) 42 (1990) 275–288;
J. Boissonade, Q. Ouyang, A. Arneodo, J. Elezgaray, J.C. Roux and P. De Kepper, in: Nonlinear Wave Processes in Excitable Media, eds. A.V. Holden, M. Markus and H.G. Othmer (Plenum, New York, 1990).

[7] Q. Ouyang, V. Castets, J. Boissonade, J.C. Roux, P. De Kepper and H.L. Swinney, J. Chem. Phys., submitted for publication.

[8] C. Vidal and A. Pacault, in: Evolution of Order and Chaos, ed. H. Haken (Springer, Berlin, 1982) p. 74.

[9] S.C. Müller, in: From Chemical to Biological Organization, eds. M. Markus, S.C. Müller and G. Nicolis (Springer, Berlin, 1988) p. 83.

[10] J.J. Tyson and J.P. Keener, Physica D 32 (1988) 327.

[11] V.I. Krinsky, in: Self-Organization of Autowaves and Structures Far from Equilibrium, ed. V.I. Krinsky (Springer, Berlin, 1984) p. 9.

[12] V.S. Zykov, Simulation of Wave Processes in Excitable Media (Manchester Univ. Press, Manchester, 1989).

[13] R.J. Field and M. Burger, eds., Oscillations and Traveling Waves in Chemical Systems (Wiley, New York, 1985).

[14] A. Pacault, Q. Ouyang and P. De Kepper, J. Stat. Phys. 48 (1987) 1005.

[15] G. Nicolis and I. Prigogine, Self-organization in Nonequilibrium Chemical Systems (Wiley, New York, 1977).

[16] H. Haken, Synergetics, an Introduction (Springer, Berlin, 1977).

[17] V. Castets, E. Dulos, J. Boissonade and P. De Kepper, Phys. Rev. Lett. 64 (1990) 2953.

[18] A.M. Turing, Phil. Trans. R. Soc. London B 327 (1952) 37.

[19] A.M. Zhabotinsky and A.N. Zaikin, J. Theor. Biol. 40 (1973) 45;
M. Orbàn, J. Am. Chem. Soc. 102 (1980) 4311;
K. Sholwalter, J. Chem. Phys. 73 (1980) 3735.

[20] P. Möckel, Naturwissenschaften 64 (1977) 224;
M. Gimenez and J.C. Micheau, Naturwissenschaften 70 (1983) 90;
D. Avnir and M. Kagan, Nature 307 (1984) 717.

[21] J.C. Micheau, M. Gimenez, P. Borckmans and G. Dewel, Nature 305 (1983) 43.

[22] I. Nagypál, G. Basza and I.R. Epstein, J. Am. Chem. Soc. 108 (1986) 3635.

[23] S. Chandrasekhar, Hydrodynamic and Hydromagnetic Stability (Oxford Univ. Press, 1961);
H.L. Swinney and J.P. Gollub, eds., Hydrodynamic Instabilities and the Transition to Turbulence (Springer, Berlin, 1981).

[24] J.D. Murray, Mathematical Biology (Springer, Berlin, 1989).

[25] P. De Kepper, I.R. Epstein, K. Kustin and M. Orbán, J. Phys. Chem. 86 (1982) 170.

[26] I. Lengyel, G. Rabai and I.R. Epstein, J. Am. Chem. Soc. 112 (1990) 4606.

[27] A.J. Indelli, J. Phys. Chem. 68 (1967) 3027;
D.M. Kern and C.-H. Kim, J. Am. Chem. Soc. 87 (1965) 5309;
J. De Meeus and J. Sigalla, J. Chim. Phys. Chim. Biol. 63 (1965) 453.

[28] O. Citri and I.R. Epstein, J. Phys. Chem. 91 (1987) 6034.

[29] I. Lengyel and I.R. Epstein, Science, submitted for publication.

[30] J.E. Pearson and W. Horsthemke, J. Chem. Phys. 90 (1989) 1588.
[31] A. Arneodo, J. Elezgaray, J. Pearson and T. Russo, Physica D 49 (1991) 141–160, these Proceedings.
[32] Q. Ouyang and H.L. Swinney, private communication (June 1990).
[33] I. Nagypál, E. Dulos, V. Castets, J. Boissonade and P. De Kepper, in preparation.
[34] D. Walgraef, G. Dewel and P. Borckmans, Adv. Chem. Phys. 49 (1982) 311.
[35] J. Boissonade, V. Castets, E. Dulos and P. De Kepper, in: Bifurcation and Chaos: Analysis, Algorithms, Applications, eds. T. Küpper, F.W. Schneider, R. Seydel and H. Troger, (Birkhäuser, Basel, 1991), p. 64.
[36] J. Elezgaray and A. Arneodo, in: New Trends in Nonlinear Dynamics and Pattern Forming Phenomena: The Geometry of Nonequilibrium, eds. P. Coullet and P. Huerre (Plenum, New York, 1990) p. 21;
A. Arneodo and J. Elezgaray, Phys. Lett. A 143 (1990) 25.
[37] W.Y. Tam and H.L. Swinney, Phys. Rev. A 36 (1989) 1211.
[38] G. Dewel, D. Walgraef and P. Borckmans, J. Chim. Phys. (Paris) 84 (1987) 1335;
G. Dewel and P. Borckmans, Phys. Lett. A 84 (1987) 1335;
G. Dewel and P. Borckmans, in: Patterns Defect and Materials Instabilities, eds. D. Walgraef and N. Ghoniem, NATO Advanced Studies (Kluwer, Dordrecht), in press.
[39] J. Boissonade, J. Phys. (Paris) 49 (1988) 541.
[40] P. De Kepper, J. Boissonade and I.R. Epstein, J. Phys. Chem. 94 (1990) 6525.
[41] H. Meinhardt, Models of Biological Patterns Formation (Academic Press, New York, 1982).
[42] A. Babloyantz, Molecules, Dynamics and Life (Wiley, New York, 1986).